SUPPLEMENTARY INFORMATION

Identification and characterization of bacterial enzymes catalyzing the synthesis of 1,8-dihydroxynaphthalene, a key precursor of dihydroxynaphthalene melanin, from *Sorangium cellulosum*

Yusuke Sone[a], Shuto Nakamura[a], Makoto Sasaki[a], Fumihito Hasebe[a], Seung-Young Kim[a], and Nobutaka Funa[a, #]

[a]Graduate Division of Nutritional and Environmental Sciences, University of Shizuoka, Shizuoka, Japan

Running Head: Enzymes catalyzing 1,8-DHN synthesis from *S. cellulosum*

Address correspondence to Nobutaka Funa, funa@u-shizuoka-ken.ac.jp

FIGURE LEGENDS FOR SUPPLEMENTAL FIGURES

Supplemental Fig S1. Phylogenetic tree of aldoketo reductase (AKR) superfamily proteins. The phylogenetic tree was constructed using CLUSTALW (http://clustalw.ddbj.nig.ac.jp) and was drawn in Njplot. For information on AKR numbering and sequences, refer to https://www.med.upenn.edu/akr/.

Supplemental Fig S2. Alignment of AKR proteins. AKR13B1 (accession number: AE003996_7) is a phenylacetaldehyde dehydrogenase from *Xylella fastidiosa*. AKR13D1 (AY766462) is a perakine reductase from *Rauvolfia serpentine*. AKR11A1 (BSU39780) and AKR11B1 (BSU09530) are putative AKRs from *Bacillus subtilis*. The conserved catalytic tetrads are highlighted by triangles.

Supplemental Fig S3. Phylogenetic tree of NTF2-like superfamily proteins. The BdsB homologs are shown as accession numbers. Accession numbers of other functionally known enzymes are also shown.

Supplemental Fig S4. Alignment of NTF2-like superfamily proteins. The putative active sites of SnoaL2 are highlighted by triangles.

Supplemental Fig S5. ^{1}H-NMR and ^{13}C-NMR spectra of scytalone (**3**).

Supplemental Fig S6. Chiral chromatography of 3,8-dihydroxy-6-methoxy-tetralone (**7**). Chromatograms of racemic-**7**, (*R*)-**7** derived from *in vivo* experiments, and (*R*)-**7** derived from *in vitro* experiments are shown in the bottom, middle, and top, respectively.

Supplemental Fig S7. *In vitro* reconstitution of 1,8-DHN (**1**) synthesis by recombinant proteins. (A) Authentic **1**. (B) Reaction of SoceCHS1, BdsA, and BdsB with malonyl-CoA and NADPH. (C) Negative control reaction of B using boiled enzymes. (D) Reaction of SoceCHS1 with malonyl-CoA. (E) Negative control reaction of D using boiled SoceCHS1.

Supplemental Fig S8. Oxidation of (*R*)-scytalone (**3**) by BdsA. (A) HPLC chromatogram of the reaction containing BdsA, (*R*)-**3**, and $NADP^+$. Flaviolin (**6**) is derived from auto-oxidation of T_4HN (**2**). (B) Negative control reaction of A using boiled BdsA.

Supplemental Fig S9. Reduction of T_3HN (**4**) by BdsA. (A) Reaction containing BdsA, **4**, and NADPH. (B) Negative control reaction of A without NADPH. (C) Negative control reaction of A using boiled BdsA.

Supplemental Fig S10. ^{1}H-NMR spectrum of vermelone (**5**). Unassigned signals are from an unknown derivative of **5**.

Supplemental Fig S11. Reduction of 1,3-DHN (**9**) by BdsA. (A) Scheme of the reduction of **9** by BdsA. (B) Reaction containing BdsA, **9**, and NADPH. (C) Negative control reaction of B using boiled BdsA. (D) Chiral HPLC chromatogram of racemic **11**. (E) Chiral HPLC chromatogram of (+)-**11**.

Supplemental Fig S12. Dehydration of vermelone (**5**) by BdsB. (A) Reaction containing BdsB and **5**. (B) Negative control reaction of A using boiled BdsB.

Supplemental Fig S13. Gene organization of *Bds* operons. Type III PKSs, AKRs, and SnoaL2-like proteins are shown in red, green, and blue, respectively.

Supplemental Fig S14. SDS-PAGE analysis of recombinant proteins. The gels were stained with Coomassie Brilliant Blue R-250.

Supplemental Fig S15. ^{1}H-NMR spectrum of 1,3,8-trihydroxynaphthalene (**4**). Unassigned signals are from an unknown derivative of **4**.

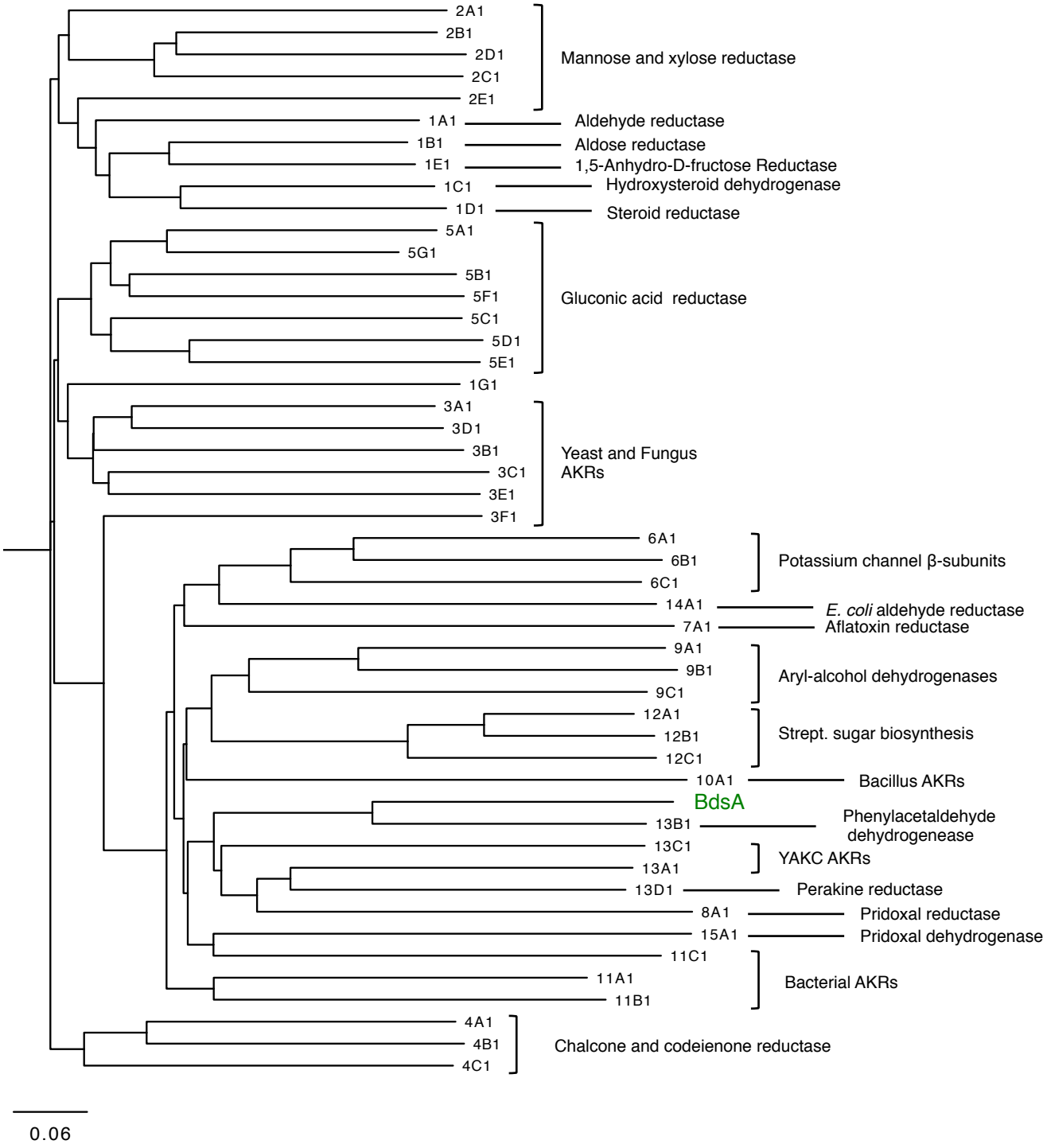
2A1
2B1
2D1
2C1
2E1
Mannose and xylose reductase
1A1
Aldehyde reductase
1B1
Aldose reductase
1E1
1,5-Anhydro-D-fructose Reductase
1C1
Hydroxysteroid dehydrogenase
1D1
Steroid reductase
5A1
5G1
5B1
5F1
5C1
5D1
5E1
Gluconic acid reductase
1G1
3A1
3D1
3B1
3C1
3E1
3F1
Yeast and Fungus AKRs
6A1
6B1
6C1
Potassium channel β-subunits
14A1
E. coli aldehyde reductase
7A1
Aflatoxin reductase
9A1
9B1
9C1
Aryl-alcohol dehydrogenases
12A1
12B1
12C1
Strept. sugar biosynthesis
10A1
Bacillus AKRs
BdsA
13B1
Phenylacetaldehyde dehydrogenease
13C1
13A1
YAKC AKRs
13D1
Perakine reductase
8A1
Pridoxal reductase
15A1
Pridoxal dehydrogenase
11C1
11A1
11B1
Bacterial AKRs
4A1
4B1
4C1
Chalcone and codeienone reductase
0.06

Figure S1

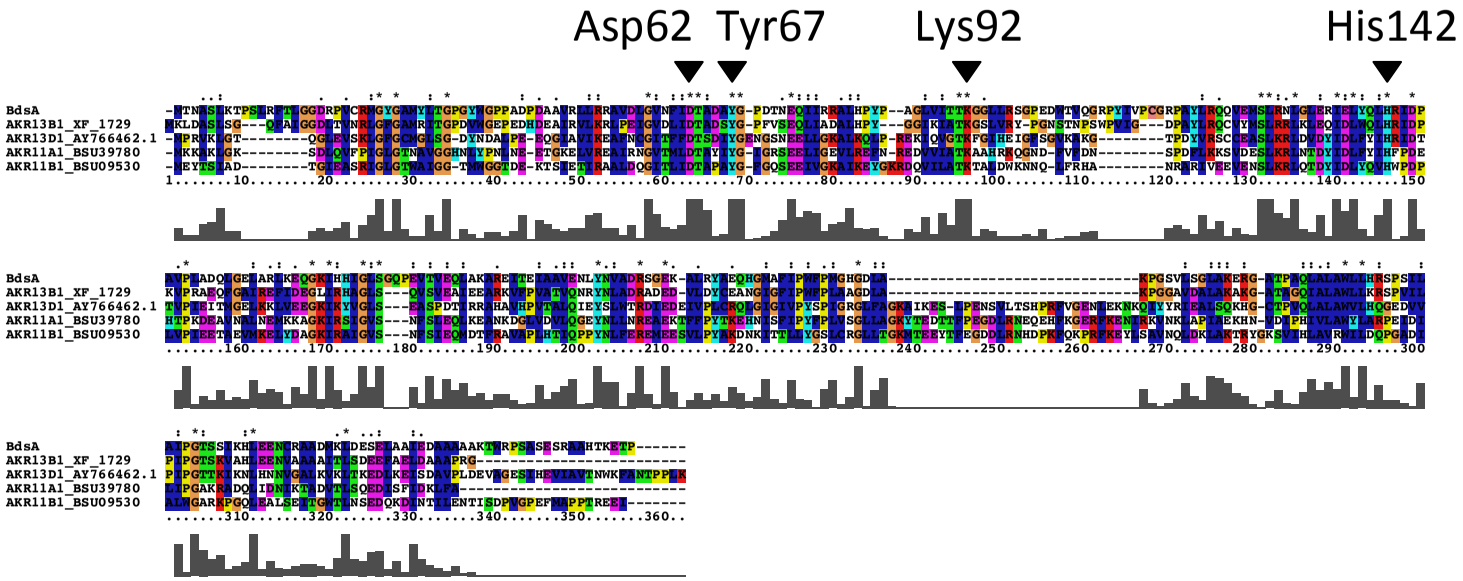
Asp62
Tyr67
Lys92
His142
BdsA
AKR13B1_XF_1729
AKR13D1_AY766462.1
AKR11A1_BSU39780
AKR11B1_BSU09530

Figure S2

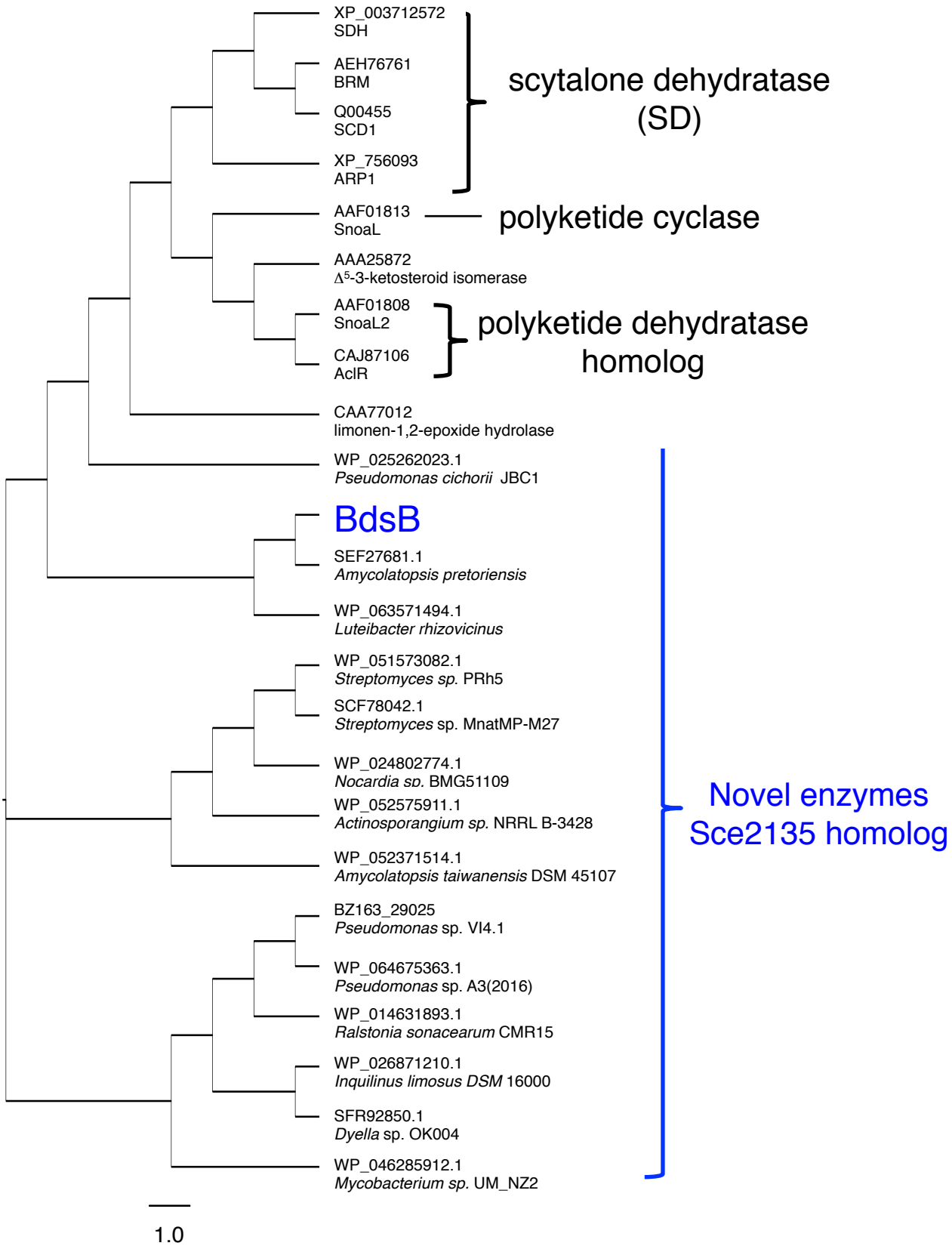
XP_003712572
SDH
AEH76761
BRM
Q00455
SCD1
XP_756093
ARP1
scytalone dehydratase
(SD)
AAF01813
SnoaL
polyketide cyclase
AAA25872
Δ5-3-ketosteroid isomerase
AAF01808
SnoaL2
CAJ87106
AclR
polyketide dehydratase
homolog
CAA77012
limonen-1,2-epoxide hydrolase
WP_025262023.1
Pseudomonas cichorii JBC1
BdsB
SEF27681.1
Amycolatopsis pretoriensis
WP_063571494.1
Luteibacter rhizovicinus
WP_051573082.1
Streptomyces sp. PRh5
SCF78042.1
Streptomyces sp. MnatMP-M27
WP_024802774.1
Nocardia sp. BMG51109
WP_052575911.1
Actinosporangium sp. NRRL B-3428
WP_052371514.1
Amycolatopsis taiwanensis DSM 45107
BZ163_29025
Pseudomonas sp. VI4.1
WP_064675363.1
Pseudomonas sp. A3(2016)
WP_014631893.1
Ralstonia sonacearum CMR15
WP_026871210.1
Inquilinus limosus DSM 16000
SFR92850.1
Dyella sp. OK004
WP_046285912.1
Mycobacterium sp. UM_NZ2
Novel enzymes
Sce2135 homolog
1.0

Figure S3

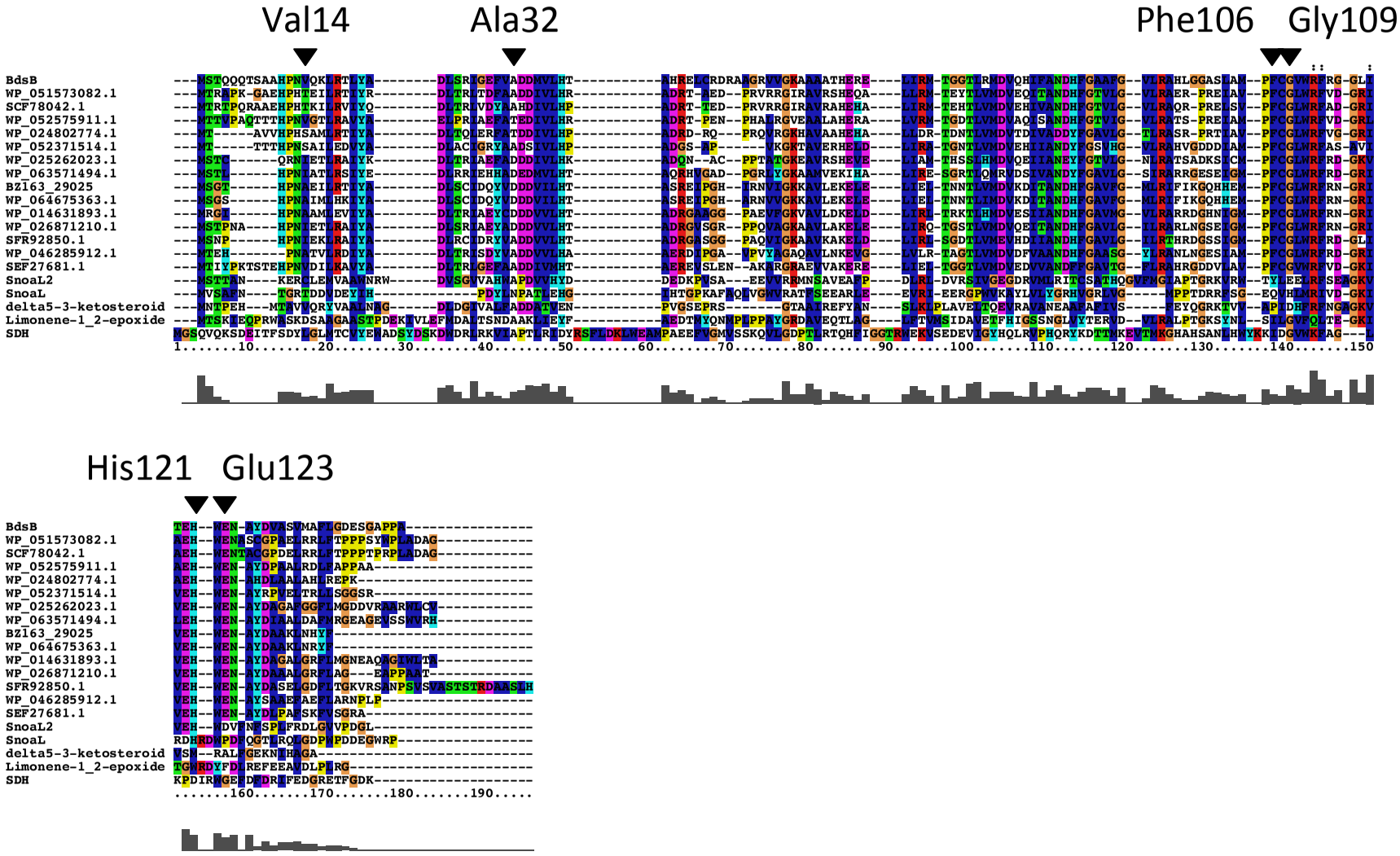
Val14
Ala32
Phe106
Gly109
His121
Glu123
BdsB
WP_051573082.1
SCF78042.1
WP_052575911.1
WP_024802774.1
WP_052371514.1
WP_025262023.1
WP_063571494.1
BZ163_29025
WP_064675363.1
WP_014631893.1
WP_026871210.1
SFR92850.1
WP_046285912.1
SEF27681.1
SnoaL2
SnoaL
delta5-3-ketosteroid
Limonene-1_2-epoxide
SDH

Figure S4

^{1}H NMR spectrum of scytalone (**3**)

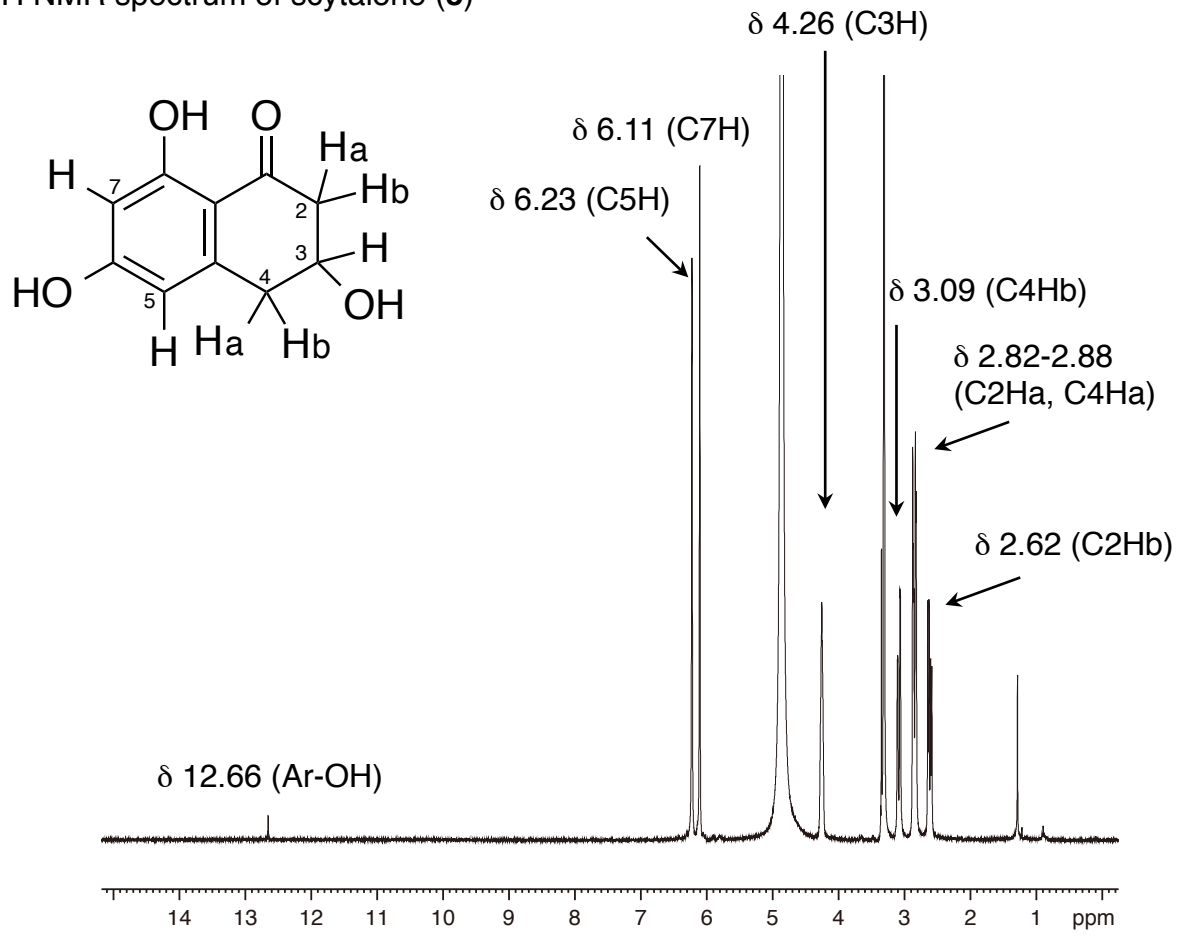

^{13}C NMR spectrum of scytalone (**3**)

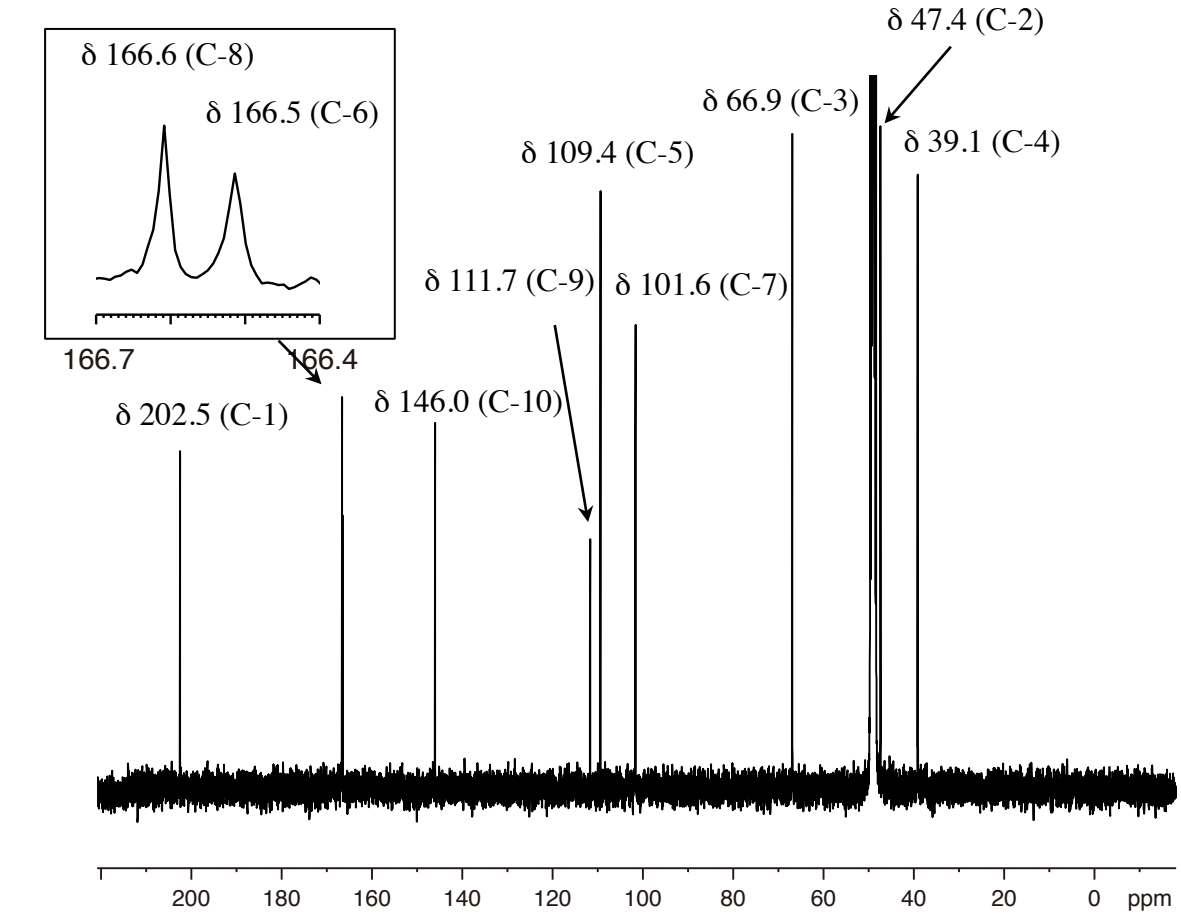

Figure S5

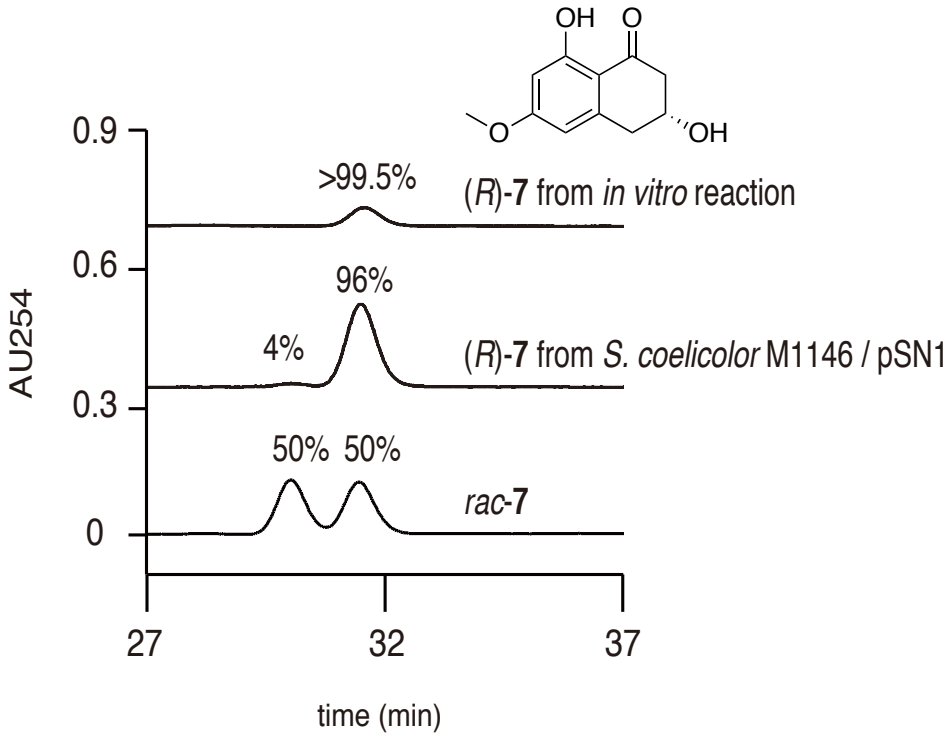
OH
O
O
OH
0.9
0.6
0.3
0
AU254
>99.5%
(R)-7 from in vitro reaction
96%
4%
(R)-7 from S. coelicolor M1146 / pSN1
50% 50%
rac-7
27
32
37
time (min)

Figure S6

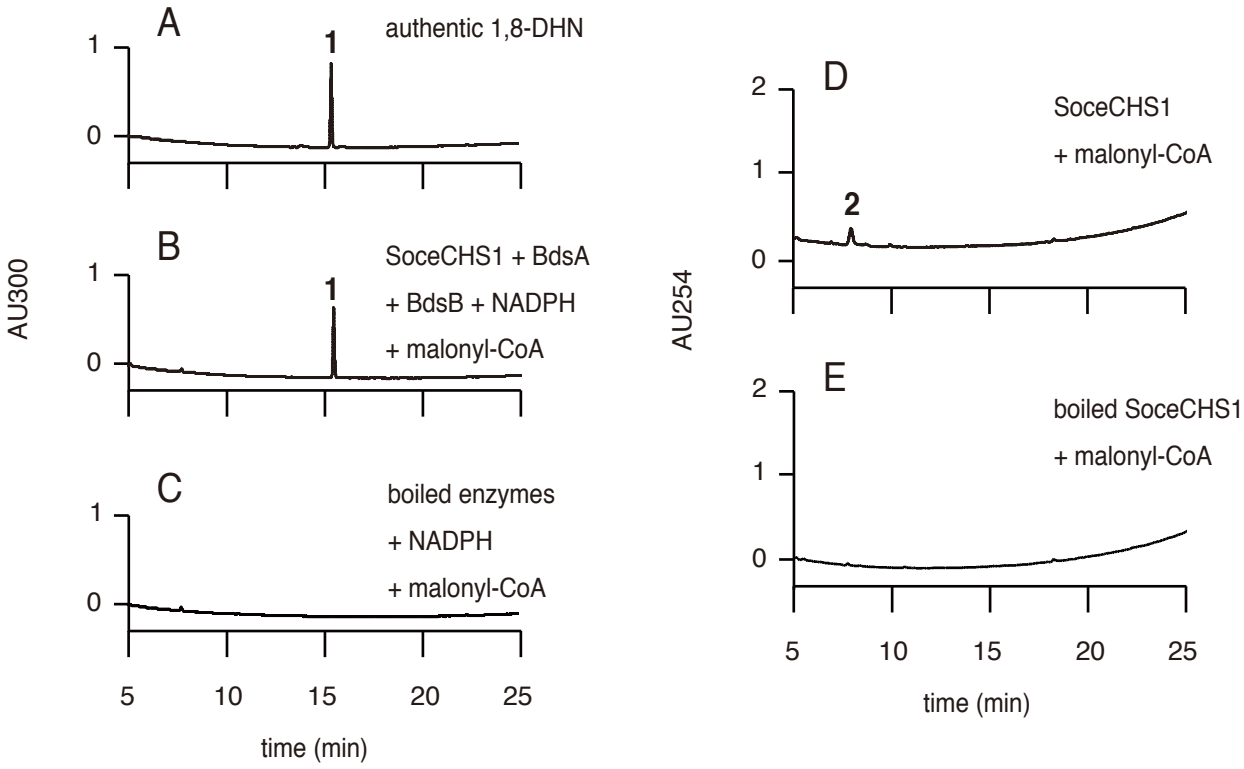
A
authentic 1,8-DHN
1
B
SoceCHS1 + BdsA
+ BdsB + NADPH
+ malonyl-CoA
C
boiled enzymes
+ NADPH
+ malonyl-CoA
AU300
time (min)
D
SoceCHS1
+ malonyl-CoA
2
E
boiled SoceCHS1
+ malonyl-CoA
AU254
time (min)

Figure S7

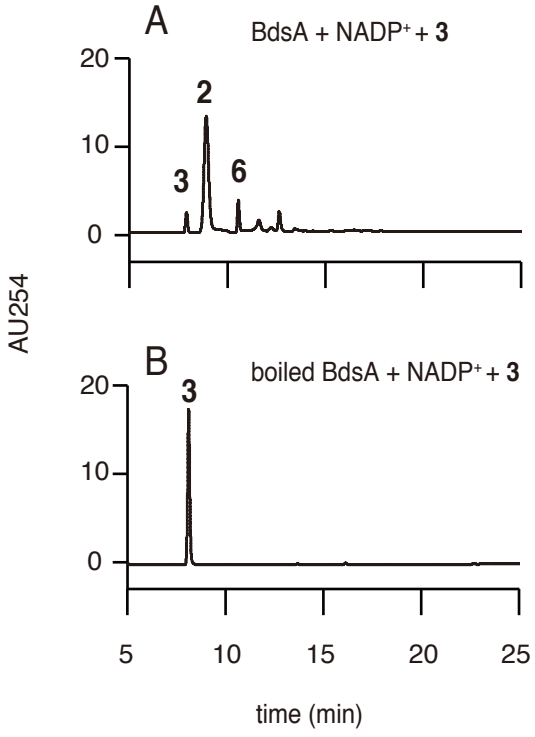
A
BdsA + NADP+ + 3
20
10
0
2
3
6
B
boiled BdsA + NADP+ + 3
20
10
0
3
AU254
5
10
15
20
25
time (min)

Figure S8

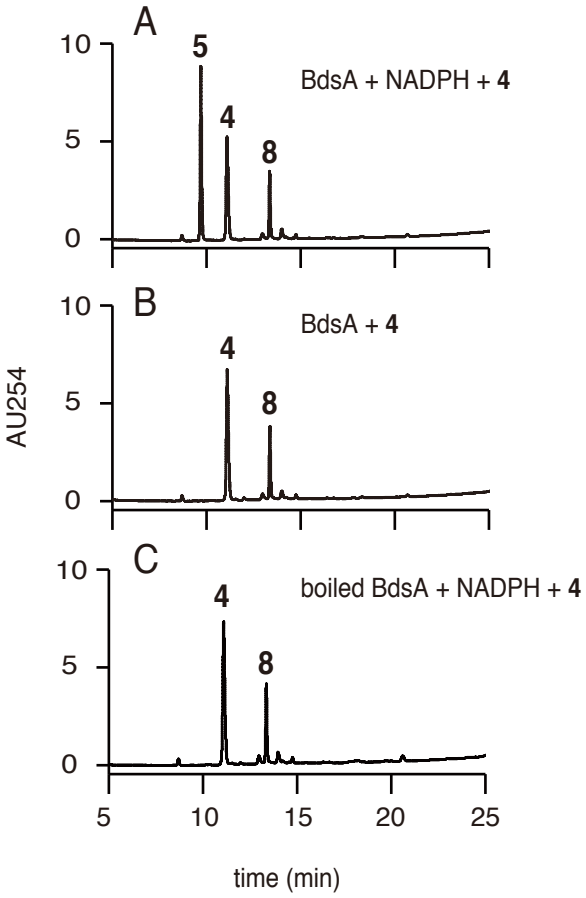
A
10
5
0
5
4
8
BdsA + NADPH + 4
B
10
5
0
4
8
BdsA + 4
C
10
5
0
4
8
boiled BdsA + NADPH + 4
AU254
5
10
15
20
25
time (min)

Figure S9

^{1}H NMR spectrum of vermelone (**5**)

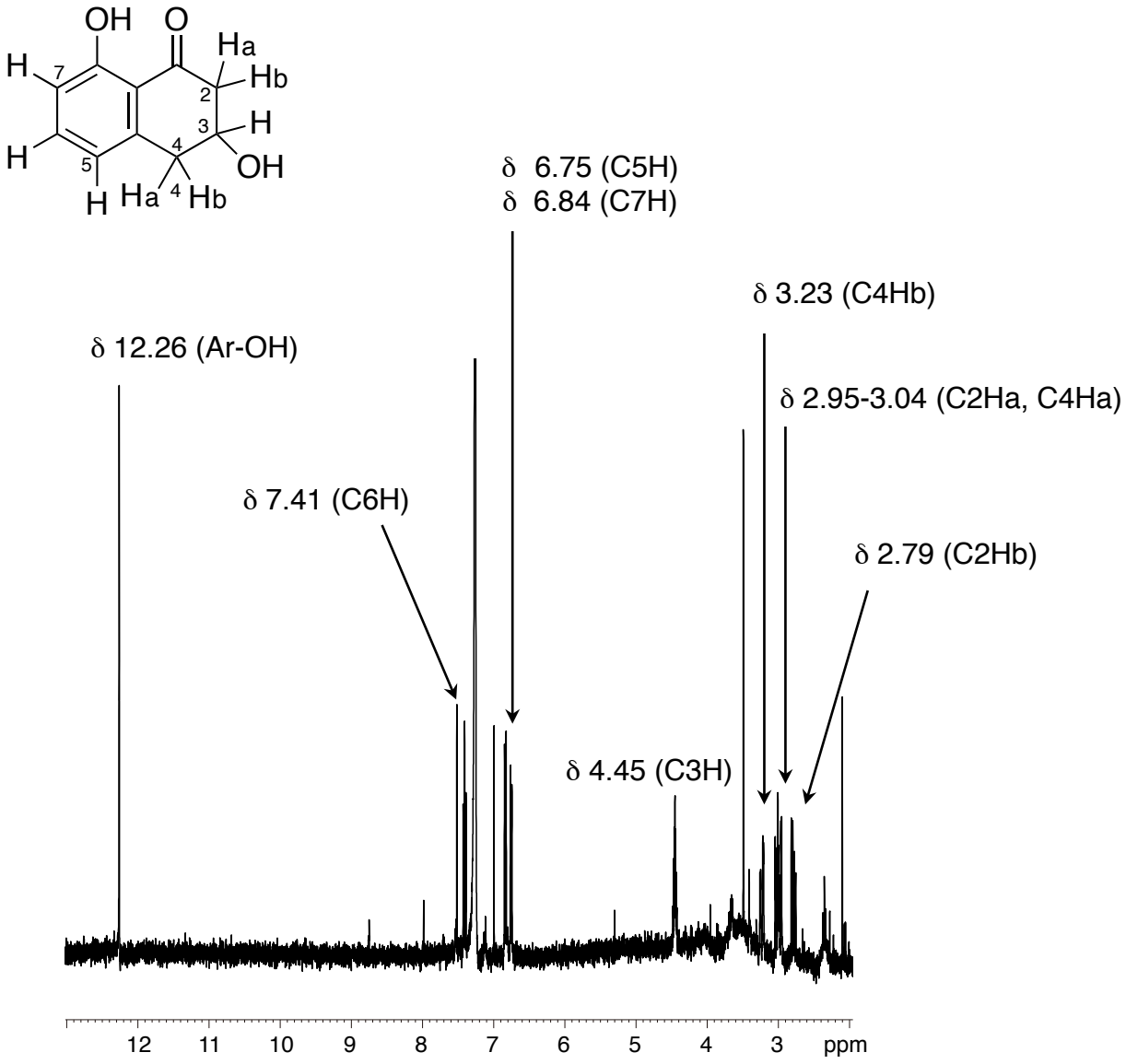

Figure S10

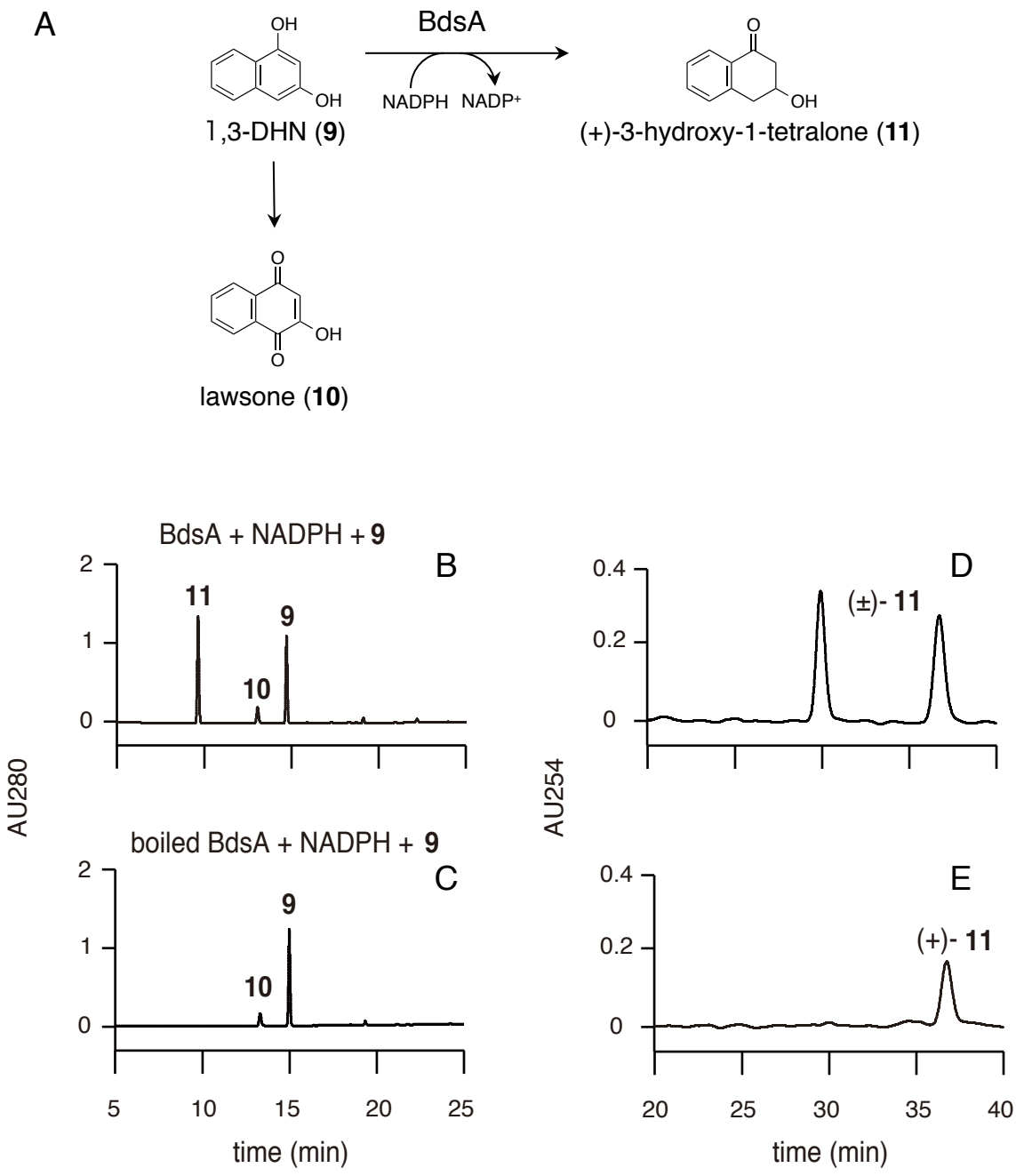
A
OH
OH
BdsA
NADPH NADP+
O
OH
1,3-DHN (9)
(+)-3-hydroxy-1-tetralone (11)
O
OH
O
lawsone (10)
BdsA + NADPH + 9
B
11
9
10
2
1
0
AU280
boiled BdsA + NADPH + 9
C
9
10
2
1
0
5
10
15
20
25
time (min)
D
0.4
0.2
0
(±)- 11
AU254
E
0.4
0.2
0
(+)- 11
20
25
30
35
40
time (min)

Figure S11

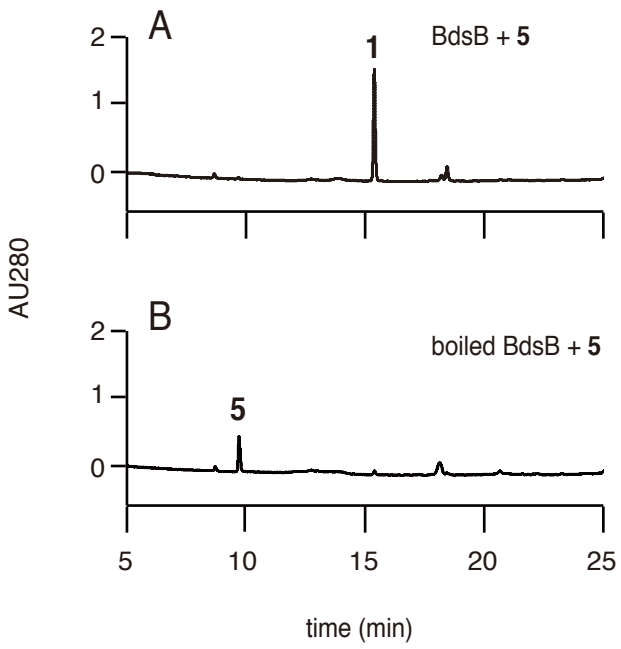

Figure S12

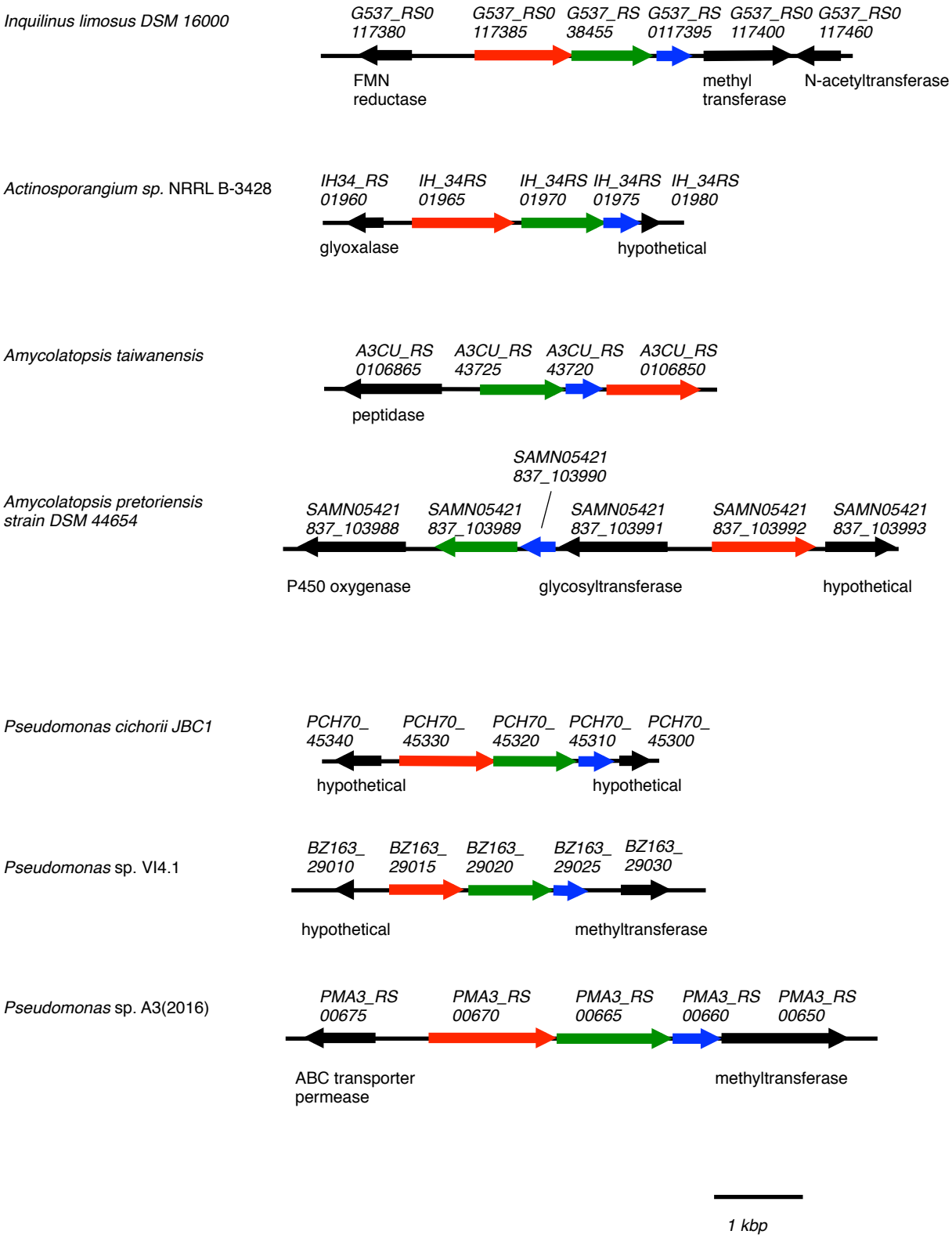
Inquilinus limosus DSM 16000
G537_RS0 117380
G537_RS0 117385
G537_RS 38455
G537_RS 0117395
G537_RS0 117400
G537_RS0 117460
FMN reductase
methyl transferase
N-acetyltransferase
Actinosporangium sp. NRRL B-3428
IH34_RS 01960
IH_34RS 01965
IH_34RS 01970
IH_34RS 01975
IH_34RS 01980
glyoxalase
hypothetical
Amycolatopsis taiwanensis
A3CU_RS 0106865
A3CU_RS 43725
A3CU_RS 43720
A3CU_RS 0106850
peptidase
Amycolatopsis pretoriensis strain DSM 44654
SAMN05421 837_103990
SAMN05421 837_103988
SAMN05421 837_103989
SAMN05421 837_103991
SAMN05421 837_103992
SAMN05421 837_103993
P450 oxygenase
glycosyltransferase
hypothetical
Pseudomonas cichorii JBC1
PCH70_ 45340
PCH70_ 45330
PCH70_ 45320
PCH70_ 45310
PCH70_ 45300
hypothetical
hypothetical
Pseudomonas sp. VI4.1
BZ163_ 29010
BZ163_ 29015
BZ163_ 29020
BZ163_ 29025
BZ163_ 29030
hypothetical
methyltransferase
Pseudomonas sp. A3(2016)
PMA3_RS 00675
PMA3_RS 00670
PMA3_RS 00665
PMA3_RS 00660
PMA3_RS 00650
ABC transporter permease
methyltransferase
1 kbp

Figure S13

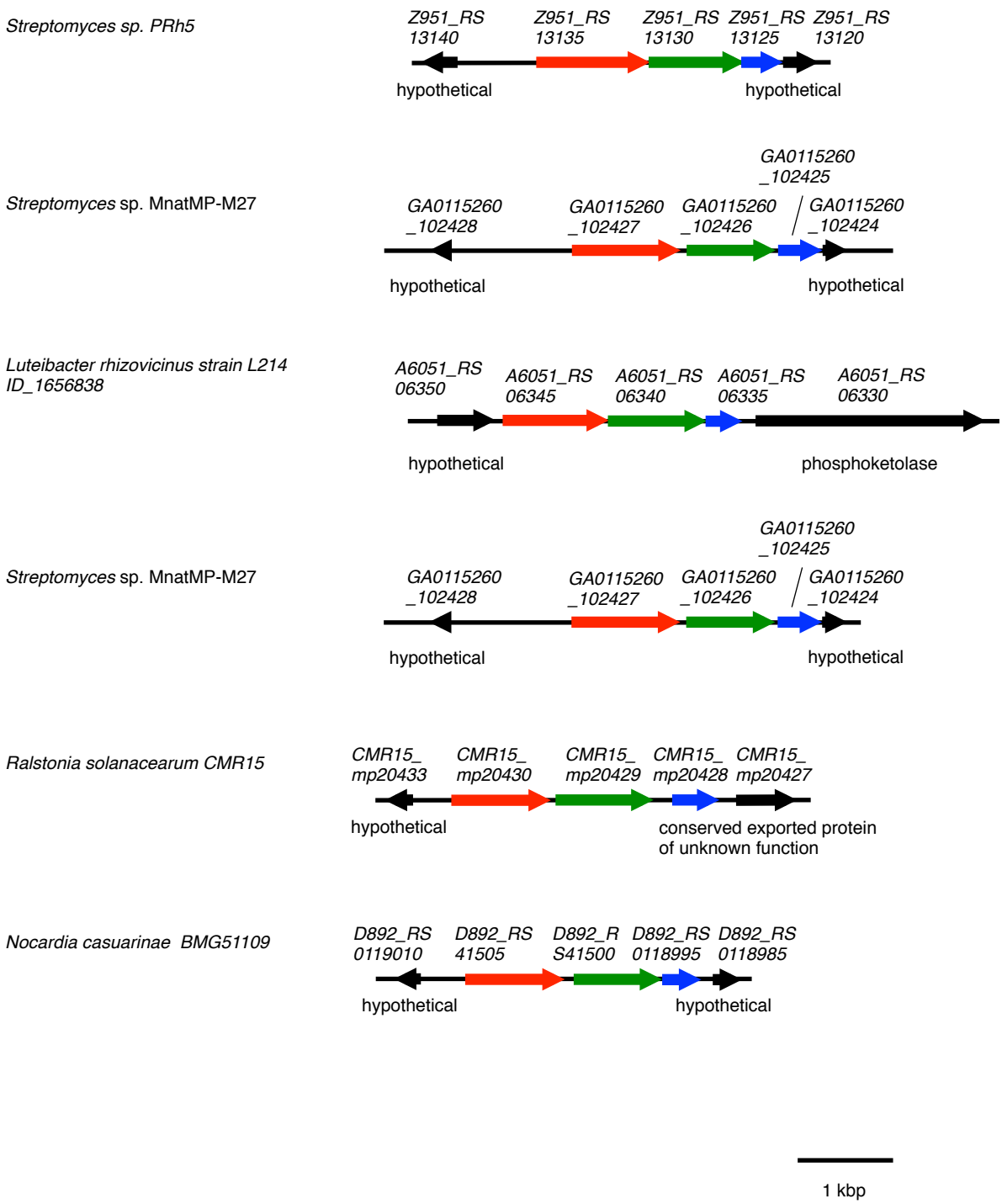

Figure S13 continued

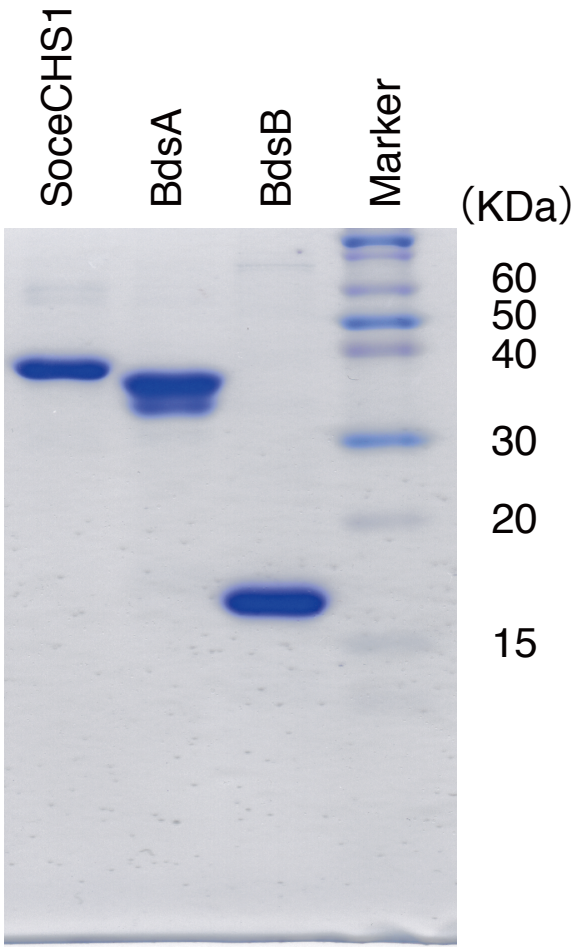

Figure S14

^{1}H NMR spectrum of 1, 3, 8-trihydroxynaphthalene (**4**)

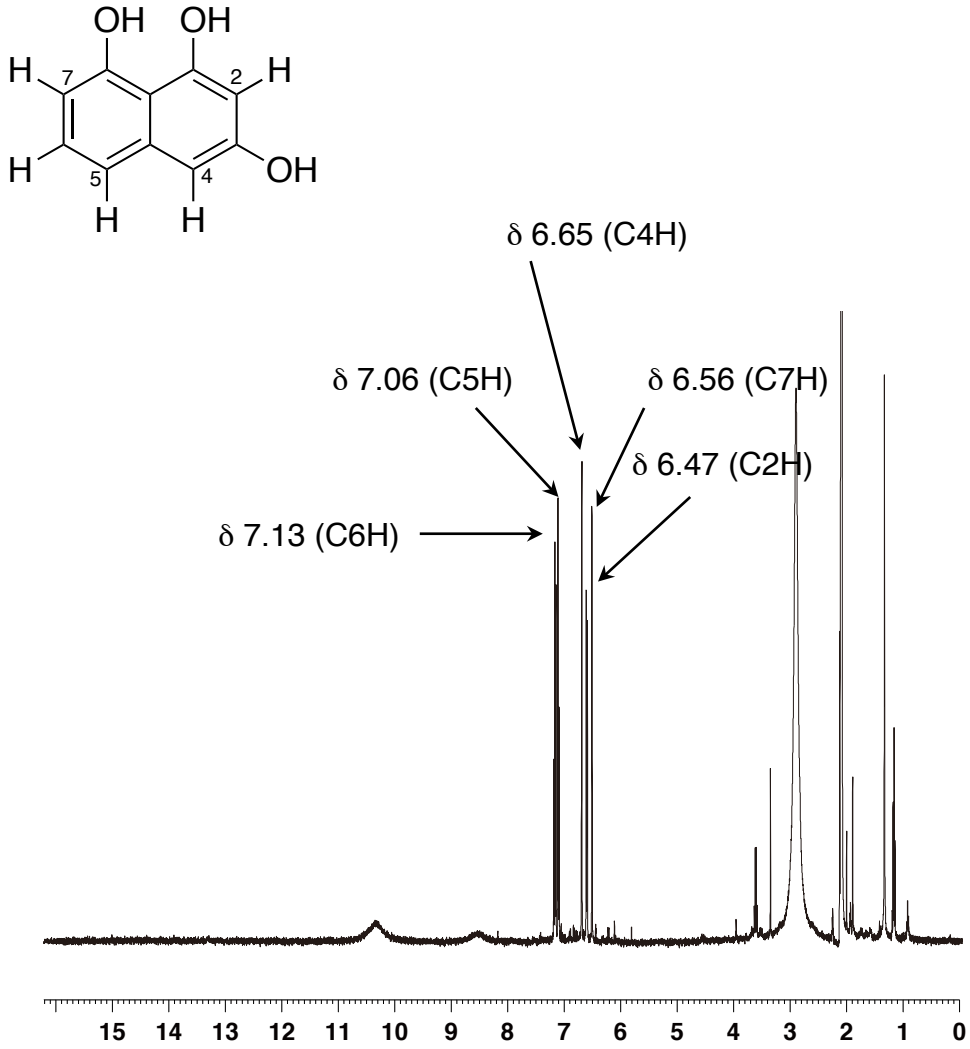

Figure S15